Non-Markovian Dynamics of the Vibrations of Ions in Water from Femtosecond Infrared Three-Pulse Photon Echoes

Peter Hamm, Manho Lim,* and Robin M. Hochstrasser
Department of Chemistry, University of Pennsylvania, Philadelphia, Pennsylvania 19104-6323
(Received 19 June 1998)

The first femtosecond three-pulse photon echo experiment of a vibrational transition is presented. A mode of the azide ion N_3^- at 2043 cm^{-1} is used to probe the impulsively excited vibrational energy distribution and hence the dynamics of the water around the ion. The vibrational frequency correlations decay on time scales of about 80 fs and 1.3 ps, while a small part remains for longer than about 10 ps. The 1.3 ps decay is the residence time for hydrogen bonds to the ion. Major differences between vibrational and optical three-pulse echoes are addressed. [S0031-9007(98)07971-X]

PACS numbers: 42.50.Md, 78.30.Cp, 82.80.Ch

It is of great interest to obtain molecular level descriptions of the structural fluctuations occurring in aqueous ionic solutions. Although the radial distributions of water associated with ions or molecules are known [1] and the structural evolutions can be simulated [2–4], this paper represents the first direct measurements of these dynamics. The fast making and breaking of bonds between water and ionic solutes implies that at each instant there is a distribution of structures and ion vibrational frequencies. The underlying dynamics is not determined by spectral line shape analysis. If the distribution were fixed for a long enough time, as at low temperatures, a conventional two-pulse photon echo experiment would measure an average dephasing time T_2 for the transitions. Fayer and co-workers [5–7] recently reported such measurements for some solution and glassy systems using picosecond pulses from a free electron laser. However, in the presence of spectral diffusion the dynamics cannot be simply described by a single T_2 parameter, but, as shown by Ippen and co-workers [8] for optical transitions, *three-pulse photon echo* measurements can yield the non-Markovian dynamics of the inhomogeneous distribution. These concepts were used widely in studies of the dynamics of electronic spectra [8–13]. This experimental and theoretical work established that a three-pulse echo reveals the correlation function of the fluctuations of the electronic energy gap, which signifies the solvent induced energy changes of the two level system. In the present paper we adapt the three-pulse echo experiment to studies in the vibrational infrared spectrum.

The character of three-pulse echoes is different for electronic and vibrational transitions. For example, it is seldom appropriate to incorporate only two levels of the system in a nonlinear infrared experiment. While the decay of electronically excited state populations is invariably very long compared with the dephasing of optical transitions, vibrational energy relaxation in small molecules and ions, strongly coupled to the bath or to other internal modes, often occurs on time scales comparable with the dephasing [14]. Another unique property of vibrations is that the fluctuations of the gaps between vibrational levels of nearly harmonic potentials, in as much as they derive from solvent induced changes in the potential energy function of the probe molecule, can be highly correlated. There is therefore much to be learned from studies of vibrational dynamics using femtosecond nonlinear spectroscopy.

In this work, asymmetric motion ν_3 of the azide ion N_3^- is issued as a probe of the dynamics of the solvent, water. Azide is a linear molecular ion with $\nu_3 = 1987$ cm^{-1} in the gas phase and 2043 cm^{-1} in D_2O. Its state-to-state time constants of energy relaxation ($1 \rightarrow 0$ and $2 \rightarrow 1$) in D_2O are $T_{10} = 2.3$ ps and $T_{21} = 1.2$ ps [15], respectively, and its anharmonicity $\Delta/\hbar c$ is 25 cm^{-1} [15,16]. The correlation functions of the spectral diffusion processes were not yet measured for any vibrational transition. In this work we not only determine the correlation function but also its structural origin in terms of motions of water molecules. The principles and methodology used in this study are expected to be quite general.

Experiment—tunable femtosecond IR pulses (duration 120 fs, energy of about 1 μJ, bandwidth about 150 cm^{-1}, frequency 2040 cm^{-1}) were generated by mixing the two outputs of a beta barium borate optical parametric amplifier in a $AgGaS_2$ crystal (see Ref. [17] for further details). The output was split into three beams with approximately equal energy (300 μJ). Two of these pulses (the pulses with direction k_1 and k_3; see Fig. 1) traversed computer controlled delay lines. The parallel polarized pulses were focused (150 μm) at the sample in the so-called box configuration [18]. The excitation density was kept small to eliminate all but third order polarization effects. The small third order signal from the solvent (<1%) was negligible compared with that from the solute. Two HgCdTe detectors recorded the signals generated in the $k_\alpha = -k_1 + k_2 + k_3$ and the $k_\beta = +k_1 - k_2 + k_3$ directions. The sample was a 50 mM solution of NaN_3 in D_2O in a CaF_2 cell (25 μm). All experiments were performed at room temperature. The linear IR spectrum was recorded as the difference between D_2O solutions of NaN_3 and NaCl at the same concentrations. This compensates for the ion induced changes in the D_2O spectrum.

 0031-9007/98/81(24)/5326(4)$15.00

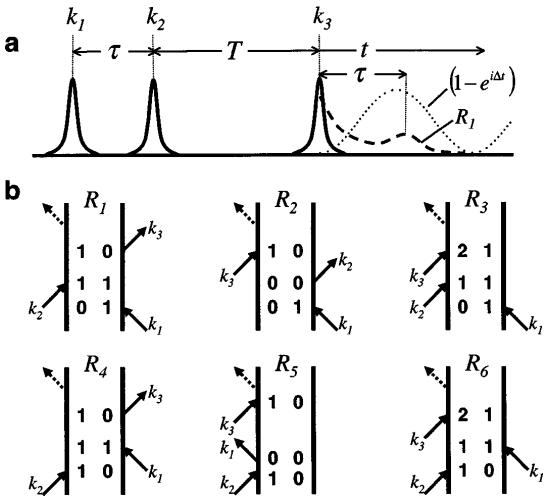

FIG. 1. (a) Time sequence of the three-pulse photon echo. The dashed line illustrates the response function R_1 ($=R_2$, detected in $-k_1 + k_2 + k_3$ direction) which shows both a free induction decay and a photon echo contribution (delayed by τ). The response function R_3 gives rise to an additional oscillatory term $(1 - e^{i\Delta t})$ (dotted line). (b) The double sided Feynman graphs, which have to be considered.

Theory—All Feynman graphs which survive the rotating wave approximation (which is valid since the bandwidth of the pulses is much smaller than their center frequency) are shown in Fig. 1(b). The detector measures the integrated four wave mixing signal,

$$S(T,\tau) = \int_0^\infty |P^{(3)}(t,T,\tau)|^2\, dt\,, \tag{1}$$

where the third order polarization $P^{(3)}$ is evaluated by convolution of the response function $\sum_i R_i(t,T,\tau)$ with the electric fields of the three laser pulses [13]. The pulse sequence t, T, τ is depicted in Fig. 1(a). The summation index i runs from 1–3 when the interaction with pulse 1 is before the interaction with pulse 2 and from 4–6 otherwise. The time T is defined as the time separation between the peaks of pulse 3 and pulse 2 for $\tau > 0$, or between the peaks of pulse 3 and pulse 1 for $\tau < 0$. The signal in the k_β direction contains the same information at $-\tau$ as the k_α signal contains at τ.

The system-bath interaction is modeled by the line shape function $g(t)$ which is the correlation function of the fluctuations $\delta\omega_{10}(t)$ and $\delta\omega_{21}(t)$ of the transition frequencies connecting the vibrational quantum states $v = 0$ and $v = 1$ or $v = 1$ and $v = 2$ [19], e.g.,

$$g(t) = \int_0^t d\tau_1 \int_0^{\tau_1} d\tau_2 \langle \delta\omega_{10}(\tau_2)\delta\omega_{10}(0)\rangle\,, \tag{2}$$

with $\omega_{10}(t) = \langle\omega_{10}(t)\rangle + \delta\omega_{10}(t)$ being the vibrational frequency modulated by solvent induced fluctuations of the potential surface.

The impulse response functions R_1, R_2, R_4, and R_5 [see Fig. 1(b)] have the same general form as those used for electronic two level systems [13], but R_3 and R_6 are three level terms,

$$\begin{aligned}
R_1 &= R_2 = \mu_{10}^4 e^{-i\omega(t-\tau)} \\
&\quad\times \exp[-g(\tau) + g(T) - g(t) - g(T+\tau) \\
&\quad - g(t+T) + g(t+T+\tau)]\,, \\
R_3 &= -\mu_{10}^2\mu_{21}^2 e^{i\Delta t} e^{-i\omega(t-\tau)} \\
&\quad\times \exp[-g(\tau) + g(T) - g(t) - g(T+\tau) \\
&\quad - g(t+T) + g(t+T+\tau)]\,, \\
R_4 &= R_5 = \mu_{10}^4 e^{-i\omega(t+\tau)} \\
&\quad\times \exp[-g(\tau) - g(T) - g(t) + g(T+\tau) \\
&\quad + g(t+T) - g(t+T+\tau)]\,, \\
R_6 &= -\mu_{10}^2\mu_{21}^2 e^{i\Delta t} e^{-i\omega(t+\tau)} \\
&\quad\times \exp[-g(\tau) - g(T) - g(t) + g(T+\tau) \\
&\quad + g(t+T) - g(t+T+\tau)]\,,
\end{aligned} \tag{3}$$

where $\Delta = \langle\omega_{10}\rangle - \langle\omega_{21}\rangle$ is the anharmonicity. A harmonic approximation for the transition dipole moments gives $2\mu_{10}^2 = \mu_{21}^2$. In deriving R_3 and R_6 it was assumed that $\delta\omega_{10}(t)$ and $\delta\omega_{21}(t)$ are strictly correlated. This implies that only the changes in the harmonic part of the ion potential are considered. In the experiment both the $v = 0 \rightarrow v = 1$ and the $v = 1 \rightarrow v = 2$ transitions are coupled to the fields, because the anharmonicity Δ is smaller than the bandwidth of the laser pulses. For this reason, the two additional Feynman graphs, R_3 and R_6, are needed. If the oscillator were treated as harmonic ($\Delta = 0$), the sum of all the graphs would vanish. Nevertheless, a nonzero response is obtained when there is anharmonicity, e.g.,

$$\sum_{i=1}^{3} R_i(t,T,\tau) = 2R_1(t,T,\tau)\,(1 - e^{i\Delta t})\,. \tag{4}$$

The second factor enhances the delayed photon echo compared with the free induction decay, as illustrated in Fig. 1(a). This term can also cause oscillations in the signal versus τ when $\Delta/2\pi$ exceeds the dephasing rate and is smaller than the inhomogeneous width. Such oscillations have been observed in glasses and liquids [6]. However, neither of these conditions are met in the present situation so that an oscillatory response is neither predicted nor observed.

Vibrational energy relaxation is taken into account through the multiplicative factors,

$$\exp\Big(-\frac{t/2 + T + \tau/2}{T_{10}}\Big) \quad \text{for } R_1, R_2, R_4, \text{ and } R_5\,, \tag{5a}$$

$$\text{and} \quad \exp\Big(-\frac{t(T_{10}+T_{21})}{2T_{10}T_{21}} - \frac{T+\tau/2}{T_{10}}\Big) \quad \text{for } R_3 \text{ and } R_6\,,$$

This phenomenology assumes that the T_{ij} are constant throughout the inhomogeneous distribution. Orientational relaxation for R_1 to R_6 is taken into account through the factor,

$$\begin{aligned}
&\langle\mu_z(0)\mu_z(\tau)\mu_z(\tau+T)\mu_z(\tau+T+t)\rangle \\
&\qquad = \Big\{\frac{1}{6} + \frac{2}{15}\, e^{-6DT}\Big\} e^{-2D(t+\tau)}\,,
\end{aligned} \tag{5b}$$

where $\langle \cdots \rangle$ is an orientational average, $\mu_z(t)$ is the projection of the transition dipole at t onto the laboratory z-axis, and $D = 0.023\ \mathrm{ps}^{-1}$ [16] is the rotational diffusion coefficient. Thus during the interval τ the signal decays like $P_1(\cos\,\theta)$ after which it decays fractionally like $P_2(\cos\,\theta)$.

The signal measured in the k_α and in the k_β directions was collected for the range $-1 < \tau < 1$ ps and $0 < T < 8$ ps. Figure 2 shows data as a function of τ for some selected times T chosen from about 55 scans. Neither the k_α nor k_β signals are symmetric in τ. Moreover, the asymmetry diminishes with T and has mostly disappeared by about 5 ps. If the system were homogeneous, the two signals at k_α and k_β would be identical, would peak at $\tau = 0$, and would decay with the dephasing time [8]. Therefore, the asymmetry measures the inhomogeneous distribution varying with T, so that the data in Fig. 2 prove that the transition is *not in the motional narrowing limit*. At early times T and $\tau > 0$, a delayed echo occurs in the k_α direction giving rise to an integrated signal which exceeds that in the nonrephasing direction k_β for each time τ. As time T increases, spectral diffusion destroys the phase memory and eventually, the response functions $\sum_{i=1}^{3} R_i(t, T, \tau)$ and $\sum_{i=4}^{6} R_i(t, T, \tau)$ would become identical, resulting in a signal which is symmetric in τ. The normalized first moment $M_1(T) = \int_{-\infty}^{\infty} \tau S(T, \tau)\, d\tau / \int_{-\infty}^{\infty} S(T, \tau)\, d\tau$ of the k_α signal is plotted versus T in Fig. 3. The first moment is a convenient measure of the asymmetry of the signal versus τ at a given value of T. In photon echoes of electronic transitions, where the signals were more symmetric around their peak (due to the similarity of dephasing time and pulse duration), the location of the peak signal on the τ axis was used as a measure of asymmetry [8–12] and the correlation function [20–22].

The nonexponential form of $M_1(T)$ suggests a model correlation function of the form,

$$\langle \Delta\omega_{10}(t)\Delta\omega_{10}(0)\rangle = \sum_{i=1}^{2} \Delta_i^2 \exp(-t/\tau_i) + \Delta_0^2 . \quad (6)$$

The global signal $S(T, \tau)$ was calculated using Eqs. (1)–(6), assuming a Gaussian shape for the pulses which had a duration of 120 fs. The complete two-dimensional data set (about 4500 data points) was fit using a nonlinear Levenberg-Marquardt algorithm yielding the five parameters: $\Delta_1 = 2.6\ \mathrm{ps}^{-1}$, $\tau_1 = 80$ fs, $\Delta_2 = 1.4\ \mathrm{ps}^{-1}$, $\tau_2 = 1.3$ ps, and $\Delta_0 = 0.3\ \mathrm{ps}^{-1}$. The calculated signal and $M_1(T)$ as obtained from the global fit are shown in Figs. 2 and 3 (solid lines), revealing an excellent agreement. No acceptable global fit could be obtained with only one exponential function in the correlation function. An essentially homogeneous part, which is modeled in Eq. (6) by the faster contribution τ_1, is indeed necessary. The product $\tau_1\Delta_1 = 0.2$ indicates that this contribution is close to the motional narrowing limit with a pure dephasing time $(\Delta_1^2\tau_1)^{-1} = 1.8$ ps, which is better determined than either parameter. The fact that $M_1(T)$ is still finite at the longest measured times implies the existence of an essentially static inhomogeneous contribution, which is taken into account by Δ_0 in Eq. (6).

The correlation function is shown in Fig. 3. Its basic features are reproduced by $M_1(T)$, which exhibits two time constants (100 fs and 1.4 ps) very close to those obtained for the correlation function from the global fit. The amplitude of the initial fast decaying part, however, is considerably reduced in $M_1(T)$.

With the same set of parameters the linear absorption spectrum was calculated according to

$$I(\omega) = 2\,\mathrm{Re}\int_0^{\infty} e^{i(\omega - \langle\omega_{10}\rangle)t} e^{-g(t) - t/2T_{10} - 2Dt}\, dt . \quad (7)$$

Figure 4 compares the measured and simulated spectra. The excellent agreement confirms the self-consistency of

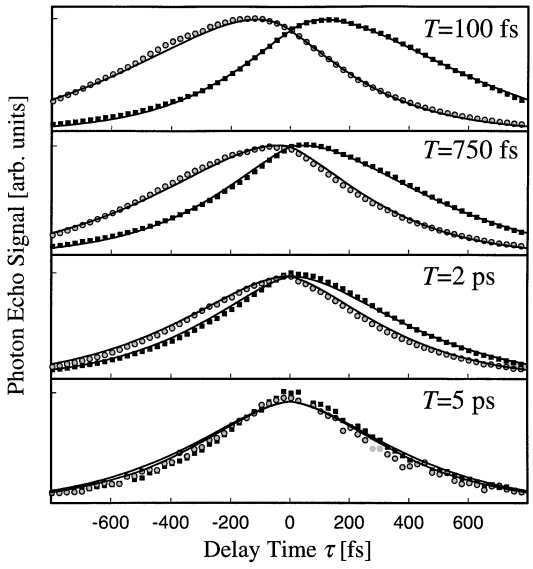

FIG. 2. Representative photon echo signals for N_3^- in D_2O at 2043 cm^{-1}, measured in the $k_\alpha = -k_1 + k_2 + k_3$ direction (black squares) and the $k_\beta = +k_1 - k_2 + k_3$ (gray circles) direction for four values of T selected from a data set of 55. The solid lines represent a global fit of all the scans to the model correlation function Eq. (6).

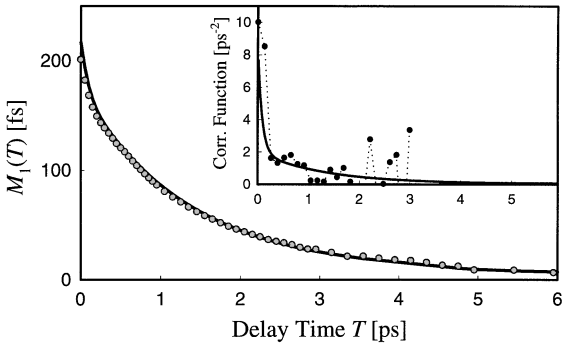

FIG. 3. The first moment $M_1(T)$ of the complete data set measured in the $-k_1 + k_2 + k_3$ direction (dots). The solid line is the function $M_1(T)$ obtained from the global fit. The insert shows the correlation function obtained from the global fit of the data (solid line) and that obtained from the experimental absorption spectrum (dots).

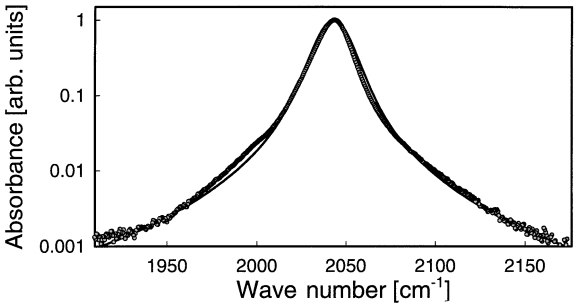

FIG. 4. Linear IR absorption spectrum of NaN_3 in D_2O (dots). The solid line shows the line shape as calculated with the parameters obtained from the global fit of the photon echo signal.

the present description [23]. Calculations of the correlation function from the measured absorption spectrum yielded the much more noisy result also shown in Fig. 3. This demonstrates the difficulties in determining the dynamics of vibrational transitions from a linear absorption spectrum.

From molecular dynamics simulations of N_3^- dissolved in water [3] the hydrogen-bond lifetime was estimated to be 1.3 ps. We have observed an inhomogeneity, which decays on precisely that time scale. Therefore, the spectral diffusion process is interpreted as fluctuations of the vibrational force constant from the making and breaking of these hydrogen bonds. There must be additional dephasing processes corresponding to the faster process in Eq. (6). These could originate from motions of negatively charged oxygen atoms sensing the positively charged central atom of N_3^- and from long range interactions. The time scale of these fluctuations (80 fs) is similar to that found for the inertial part of the water nuclear response function [24]. The total correlation function measured in our experiment is *not* the nuclear response function of pure water, but reflects the dynamics of the ion-water complex. This is another essential difference between IR and optical photon echo experiments.

The line shape function $g(t)$ is assumed to be real since no time dependent spectral shift (equivalent to the Stokes shift of an electronic transition [13]) was yet seen in pump-probe experiments of vibrational transitions. However, in this case the mixed mode anharmonicity of the ion and its associated solvent can cause the differences between the $v = 0$ and $v = 1$ states necessary for a small dynamic spectral shift. Although the average dipole moment of N_3^- is zero, there are energy fluctuations of the solvent electric field gradient that couple to the large quadrupole moment of the ion, which depends on the quantum state. For those reasons there should be a time dependent frequency shift evolving on a 1.3 ps time scale and hence a small imaginary part of $g(t)$. This will be addressed by future experiments.

The research was supported by the NSF, DFG, and NIH and used instrumentation developed from NIH Grant No. RR01348.

*Present address: Department of Chemistry, College of Natural Science, Pusan National University, Jang-Jeon Dong, Jang-Jeon Dong, Keum-Jeong Ku, Pusan 609-735, Republic of Korea.

[1] D. H. Powell, A. C. Barnes, J. E. Enderby, G. W. Neilson, and P. S. Salmon, Faraday Discuss. Chem. Soc. **85**, 137 (1988).
[2] M. Ferrario, I. R. McDonald, and M. C. R. Symons, Mol. Phys. **77**, 617 (1992).
[3] M. Ferrario, M. L. Klein, and I. R. McDonald, Chem. Phys. Lett. **213**, 537 (1993).
[4] R. Rey and J. T. Hynes, J. Chem. Phys. **108**, 142 (1998).
[5] D. Zimdars, A. Tokmakoff, S. Chen, S. R. Greenfield, M. D. Fayer, T. L. Smith, and H. A. Schwettman, Phys. Rev. Lett. **70**, 2718 (1993).
[6] K. D. Rector, A. S. Kwok, C. Ferrante, A. Tokmakoff, C. W. Rella, and M. D. Fayer, J. Chem. Phys. **106**, 10027 (1997).
[7] K. D. Rector and M. D. Fayer, J. Chem. Phys. **108**, 1794 (1998).
[8] S. D. Silvestri, A. M. Weiner, J. G. Fujimoto, and E. P. Ippen, Chem. Phys. Lett. **112**, 195 (1984).
[9] G. R. Fleming and M. Cho, Annu. Rev. Phys. Chem. **47**, 109 (1996).
[10] T. Joo and A. C. Albrecht, Chem. Phys. **176**, 223 (1993).
[11] P. Vöhringer, D. Arnett, R. Westervelt, M. Fedlstein, and N. F. Scherer, J. Chem. Phys. **102**, 4027 (1995).
[12] M. F. Emde, A. Baltuska, A. Kummrow, M. S. Pshenichnikov, and D. A. Wiersma, Phys. Rev. Lett. **80**, 4645 (1998).
[13] S. Mukamel, *Principles of Nonlinear Optical Spectroscopy* (Oxford University, New York, 1995).
[14] J. Owrutsky, D. Raftery, and R. M. Hochstrasser, Annu. Rev. Phys. Chem. **45**, 519 (1994).
[15] P. Hamm, M. Lim, and R. M. Hochstrasser, "Ultrafast XI," edited by T. Elsaesser, D. Wiersma, W. Zinth, and J. G. Fujimoto (Springer, Berlin, to be published).
[16] M. Li, J. Owrutsky, M. Sarisky, J. P. Culver, A. Yodh, and R. M. Hochstrasser, J. Chem. Phys. **98**, 5499 (1993).
[17] P. Hamm, M. Lim, and R. M. Hochstrasser, J. Chem. Phys. **107**, 10523 (1997).
[18] M. D. Levenson and S. S. Kano, *Introduction to Nonlinear Laser Spectroscopy* (Academic, Boston, 1988).
[19] D. W. Oxtoby, D. Levensque, and J. J. Weiss, J. Chem. Phys. **68**, 5528 (1978).
[20] T. Joo, Y. Jia, J.-Y. Yu, M. J. Lang, and G. F. Fleming, J. Chem. Phys. **104**, 6089 (1996).
[21] M. Cho, J.-Y. Yu, T. Joo, Y. Nagasawa, S. A. Passino, and G. R. Fleming, J. Phys. Chem. **100**, 11 944 (1996).
[22] W. P. de Boeij, M. S. Pshenichnikov, and D. A. Wiersma, Chem. Phys. Lett. **253**, 53 (1996).
[23] The small shoulder at the low frequency side of the spectrum appears to be $^{14}N^{15}N^{14}N^-$. Both the relative intensity (0.4%) and shift (-43 cm^{-1}) [P. Botschwina J. Chem. Phys. **85**, 4591 (1986)] support this assignment. The (-11 cm^{-1}) shift of $^{15}N^{14}N^{14}N^-$, on the other hand, is too small to be resolved.
[24] R. Jimenez, G. R. Fleming, P. V. Kumar, and M. Maroncelli, Nature (London) **369**, 471 (1994).